

A multifunctional GH39 glycoside hydrolase from the anaerobic gut fungus *Orpinomyces* sp. strain C1A

Jessica M Morrison¹, Mostafa S Elshahed¹, Noha Youssef^{Corresp. 1}

¹ Department of Microbiology and Molecular Genetics, Oklahoma State University, Stillwater, OK, USA

Corresponding Author: Noha Youssef
Email address: noha@okstate.edu

Background. The anaerobic gut fungi (phylum Neocallimastigomycota) represent a promising source of novel lignocellulolytic enzymes. Here, we report on the cloning, expression, and characterization of a glycoside hydrolase family 39 (GH39) enzyme (Bgxg1) that is highly transcribed by the anaerobic fungus *Orpinomyces* sp. strain C1A under different growth conditions. This represents the first study of a GH39-family enzyme from the anaerobic fungi.

Methods. Using enzyme activity assays, we performed a biochemical characterization of Bgxg1 on a variety of substrates over a wide range of pH and temperature values to identify the optimal enzyme conditions and the specificity of the enzyme. In addition, substrate competition studies and comparative modeling efforts were completed.

Results. Contrary to the narrow range of activities (β -xylosidase or α -L-iduronidase) observed in previously characterized GH39 enzymes, Bgxg1 is unique in that it is multifunctional, exhibiting strong β -xylosidase, β -glucosidase, β -galactosidase activities (11.5 ± 1.2 , 73.4 ± 7.15 , and 54.6 ± 2.26 U/mg, respectively) and a weak xylanase activity (10.8 ± 1.25 U/mg), as compared to previously characterized enzymes. Further, Bgxg1 possesses extremely high affinity (as evident by the lowest K_m values), compared to all previously characterized β -glucosidases, β -galactosidases, and xylanases. Physiological characterization revealed that Bgxg1 is active over a wide range of pH (3-8, optimum 6) and temperatures (25-60°C, optimum 39°C), and possesses excellent temperature and thermal stability. Substrate competition assays suggest that all observed activities occur at a single active site. Using comparative modeling and bioinformatics approaches, we putatively identified ten amino acid differences between Bgxg1 and previously biochemically characterized GH39 β -xylosidases that we speculate could impact active site architecture, size, charge, and/or polarity.

Discussion. Collectively, the unique capabilities and multi-functionality of Bgxg1 render it an excellent candidate for inclusion in enzyme cocktails mediating cellulose and hemicellulose saccharification from lignocellulosic biomass.

A multifunctional GH39 glycoside hydrolase from the anaerobic gut fungus *Orpinomyces* sp. strain C1A

Jessica M. Morrison¹, Mostafa S. Elshahed¹, and Noha H. Youssef^{1*}

¹Department of Microbiology and Molecular Genetics, Oklahoma State University, Stillwater, OK, USA

Author Information:

Jessica M. Morrison, Ph.D.
1110 S. Innovation way, Stillwater, Oklahoma 74074 USA.
jessica.morrison@okstate.edu

Mostafa S. Elshahed, Ph.D.
1110 S. Innovation way, Stillwater, Oklahoma 74074 USA.
mostafa@okstate.edu

***Corresponding author.**

Noha H. Youssef, Ph.D.
1110 S. Innovation way, Stillwater, Oklahoma 74074 USA.
Phone: 1-405-744-1192, Fax: 1-405-744-1112
Noha@Okstate.edu

Keywords: Anaerobic gut fungi, GH39, β -glucosidase, β -xylosidase, β -galactosidase
Short Title: Triple oligosaccharide hydrolase activity from a rumen fungus GH39 enzyme

40 **Abstract**

41 **Background.** The anaerobic gut fungi (phylum Neocallimastigomycota) represent a promising
 42 source of novel lignocellulolytic enzymes. Here, we report on the cloning, expression, and
 43 characterization of a glycoside hydrolase family 39 (GH39) enzyme (Bgxg1) that is highly
 44 transcribed by the anaerobic fungus *Orpinomyces* sp. strain C1A under different growth
 45 conditions. This represents the first study of a GH39-family enzyme from the anaerobic fungi.

46 **Methods.** Using enzyme activity assays, we performed a biochemical characterization of Bgxg1
 47 on a variety of substrates over a wide range of pH and temperature values to identify the optimal
 48 enzyme conditions and the specificity of the enzyme. In addition, substrate competition studies
 49 and comparative modeling efforts were completed.

50 **Results.** Contrary to the narrow range of activities (β -xylosidase or α -L-iduronidase) observed in
 51 previously characterized GH39 enzymes, Bgxg1 is unique in that it is multifunctional, exhibiting
 52 strong β -xylosidase, β -glucosidase, β -galactosidase activities (11.5 ± 1.2 , 73.4 ± 7.15 , and $54.6 \pm$
 53 2.26 U/mg, respectively) and a weak xylanase activity (10.8 ± 1.25 U/mg), as compared to
 54 previously characterized enzymes. Further, Bgxg1 possesses extremely high affinity (as evident
 55 by the lowest K_m values), compared to all previously characterized β -glucosidases, β -
 56 galactosidases, and xylanases. Physiological characterization revealed that Bgxg1 is active over a
 57 wide range of pH (3-8, optimum 6) and temperatures (25-60°C, optimum 39°C), and possesses
 58 excellent temperature and thermal stability. Substrate competition assays suggest that all
 59 observed activities occur at a single active site. Using comparative modeling and bioinformatics
 60 approaches, we putatively identified ten amino acid differences between Bgxg1 and previously
 61 biochemically characterized GH39 β -xylosidases that we speculate could impact active site
 62 architecture, size, charge, and/or polarity.

63 **Discussion.** Collectively, the unique capabilities and multi-functionality of Bgxxg1 render it an
 64 excellent candidate for inclusion in enzyme cocktails mediating cellulose and hemicellulose
 65 saccharification from lignocellulosic biomass.

Introduction

The production of biofuels from lignocellulosic biomass is a global priority, necessitated by the continuous depletion of recoverable fossil fuel reserves, the deleterious impact of fossil fuels on air quality, as well as their contribution to global climate change (Hill et al. 2006; National Research Council 2011; Ragauskas et al. 2006). Lignocellulosic biomass represents a vastly underutilized and largely untapped source of energy, and its mass utilization for biofuel production is one of the goals enacted by the U.S. Congress-implemented Renewable Fuel Standard (RFS), aiming to generate 16 billion gallons of biofuel from lignocellulosic sources by 2022 (National Research Council 2011).

The most frequently used method of biofuel production from lignocellulosic biomass is the enzymatic conversion of cellulose and hemicellulose polymers into sugar monomers/oligomers that could subsequently be converted into biofuels using dedicated sugar metabolizers (Elshahed 2010; Hill et al. 2006; Kumar et al. 2008). Historically, enzymatic cocktails designed for the breakdown of lignocellulosic biomass focused primarily on cellulose degradation, due to its relative structural simplicity and uniformity across all types of plant biomass. Nevertheless, the hemicellulose components in lignocellulosic biomass should not be ignored, as hemicellulose represents 20-35% of the composition of lignocellulosic biomass (Liu et al. 2008). Unlike cellulose, plant hemicelluloses are structurally more complex, with multiple types of major hemicelluloses (arabinoxylans/ glucuronoarabinoxylans, glucomannans/galactoglucomannans, mixed glucans, and xyloglucans) present in various plants (Scheller & Ulvskov 2010). The most common type of hemicellulose are the arabinoxylans/ glucuronoarabinoxylans that possess a structural backbone of β -1,4-linked xylose units (Scheller & Ulvskov 2010). Xylan degradation requires the consorted action of the endo-acting- β -1,4-xylanases and the oligosaccharide

depolymerizing β -xylosidases, among other enzymes (Elshahed 2010; Scheller & Ulvskov 2010).

The identification and characterization of novel enzymes and enzyme cocktails with superior lignocellulosic biomass saccharification properties (e.g. high substrate affinity and specific activity, activity retention at a wide range of pH and temperatures, and thermal and pH stability) signify essential thrusts in biofuel research. Members of the anaerobic gut fungi (phylum Neocallimastigomycota) represent a promising, and largely untapped, source of biomass-degrading enzymes (Ljungdahl 2008; Wang et al. 2013). Members of the Neocallimastigomycota are found in the herbivorous gut, where they are responsible for the initial colonization and degradation of plant materials ingested by their hosts (Ljungdahl 2008; Wang et al. 2013). While anaerobic gut fungi were initially discovered in sheep, they have since been found in the rumen and alimentary tracks of both ruminant and non-ruminant mammalian and reptilian herbivores (Youssef et al. 2013). The anaerobic gut fungi are excellent biomass degraders, capable of fast, efficient, and simultaneous degradation of the cellulolytic and hemicellulolytic fraction of various plants, including most common lignocellulosic biomass substrates (e.g. Corn Stover, Switchgrass, Sorghum, Energy Cane, and Alfalfa) (Borneman et al. 1989; Harhangi et al. 2003; Liggenstoffer et al. 2014; Youssef et al. 2013). Nevertheless, there have been extensive efforts dedicated to bioprospecting novel cellulases and hemicellulases from aerobic fungi (such as *Aspergillus* (Kumar & Ramon 1996; vanPeij et al. 1997), *Trichoderma* (Matsuo & Yasui 1984)), anaerobic prokaryotes (such as *Clostridium* (Bronnenmeier & Staudenbauer 1988) and *Thermoanaerobacterium* (Shao et al. 2011)) and metagenomic sequence data (Brennan et al. 2004; Hess et al. 2011); in comparison to these numerous efforts, the

identification, expression, and characterization of such enzymes from anaerobic fungi has not been as well represented in the literature (Borneman et al. 1989; Harhangi et al. 2003).

We aim to explore the utility of the anaerobic gut fungus *Orpinomyces* sp. strain C1A (henceforth referred to as C1A) as a novel source of lignocellulolytic enzymes. C1A is an isolate from the feces of an Angus steer on cellobiose-switchgrass media (Youssef et al. 2013). Our approach depends on implementing a transcriptomics-guided strategy to identify carbohydrate-active enzymes (CAZyme) transcripts that are highly expressed by C1A when grown on lignocellulosic biomass substrates as candidates for cloning, expression, and characterization. Here, we describe our efforts in cloning, expression, and characterization of one such enzyme: a GH39 transcript bioinformatically annotated as a β -xylosidase, designated Bgxgl, representing the first study of a GH39-family enzyme from anaerobic fungi. Our results document the high affinity, high specific activity, wide pH and temperature ranges, high thermal and pH stability of this enzyme, and novel multiple activities.

Materials and Methods

Transcriptomics-guided selection of a GH39 enzyme for cloning and characterization.

As a part of an extensive transcriptomic analysis of lignocellulosic biomass degradation by the anaerobic fungal isolate *Orpinomyces* sp. strain C1A (Couger et al. 2015), the most highly transcribed gene annotated as a β -xylosidase was selected for cloning and biochemical characterization. The selected m.21910 transcript (GenBank accession number KT997999) was annotated as member of the GH39 CAZyme family based on the presence of the conserved protein domain pfam01229 (Glyco_hydro_39) family. When strain C1A was grown on different substrates (glucose, Corn Stover, Energy Cane, Switchgrass, and Sorghum), m.21910 constituted 58-84% of the transcriptional activity (i.e. normalized FPKM values) of all GH39 transcripts

(n=9), and 5.7-18.2% of the transcriptional activities of all C1A genes putatively annotated as β -xylosidases (members of GH39 and GH43, n=41) (Couger et al. 2015). The gene encoding for Bgxxg1 protein was previously identified in the genome of strain C1A (GenBank contig accession number ASRE01002650.1, range: 2346-3460, see GCA_000412615.1 for whole genome). The ctg7180000059688.1 gene consists of 1115 bp and no introns (refer to IMG gene ID 2518718918 for a visual representation of the gene, https://img.jgi.doe.gov/cgi-bin/m/main.cgi?section=TaxonDetail&page=taxonDetail&taxon_oid=2518645524). The protein product is predicted to be extracellular and non-cellulosomal, based on the presence of a signal peptide, and the absence of a CBM fungal dockerin domain, respectively.

Bgxxg1 sequence analysis and phylogeny.

To determine the phylogenetic affiliation of Bgxxg1 and the overall topology and global phylogeny of GH39 CAZymes, GH39 β -xylosidase sequences available in CAZY database (http://www.cazy.org/GH39_all.html) (n=1145 total GH39 sequences, retrieved October 28, 2015, edited to remove α -iduronidases and duplicates, resulting in n=200 β -xylosidases), in addition to Bgxxg1, were aligned using Clustal Omega (Sievers et al. 2011). The generated alignment was used to construct a maximum likelihood tree in RAxML (Stamatakis 2014), which was subsequently visualized and annotated using Mega6 (Sievers et al. 2011; Tamura et al. 2013).

Synthesis, cloning, expression, and purification of Bgxxg1 protein.

bgxxg1 gene synthesis and cloning. A fraction (939 bp, positions 67-1035) of m.21910 transcript was codon optimized for ideal expression in *E. coli* (see Fig. S1 for the alignment of the original gene and codon-optimized gene), and the *bgxxg1* insert was synthesized by a commercial provider and inserted into a pET28a(+) plasmid (GenScript, Piscataway, NJ). The plasmid, pET28a(+)-

bgxgI, harbors kanamycin resistance (*kan*) and *NdeI* and *XhoI* restriction sites for selection and cloning. The pET28a(+)-*bgxgI* plasmid was first transformed into One-Shot Chemically Competent Top10 *E. coli* cells (Invitrogen, Carlsbad, CA), and the transformants were grown overnight on LB-kanamycin agar (15 µg/mL) for selection. The purified plasmid was electroporated into a protease-deficient BL21(DE3)pLysS *E. coli* strain (Novagen, EMD Millipore, Darmstadt, Germany), possessing an additional chloramphenicol resistance (*cm*) marker, using a single pulse of 1.8 kV in 0.1 cm electrocuvettes. Transformants were grown on LB agar using both kanamycin (15 µg/mL) and chloramphenicol (34 µg/mL) for selection and screened for the presence of correctly sized inserts via colony PCR using T7 forward and reverse primers.

BgxgI expression and purification. Ten milliliters of overnight cultures of BL21(DE3)pLysS *E. coli* cells transformed with pET28a(+)-*bgxgI* were used to inoculate 1 L LB broth, containing kanamycin (15 µg/mL) and chloramphenicol (34 µg/mL). The culture was incubated at 37°C with shaking at 200 rpm until an OD₆₀₀ = 0.6 was reached. Isopropyl-β-D-thiogalactopyranoside (IPTG, 1mM final concentration) was then added to induce protein production, and the culture was gently shaken at room temperature overnight. Cells were then pelleted by centrifugation (6,000 x g, 10 minutes, 4°C) and the pellets were collected and stored at -20°C.

Preliminary small-scale experiments indicated that the protein is expressed in the inclusion body fraction (Fig. S2). Inclusion body extraction was initiated by incubating the cultures in B-Per Cell Lysis Reagent (Thermo Scientific, Grand Island, NY) (10 ml per 500 ml of culture) for 15 minutes at room temperature with gentle shaking to lyse the cells. The homogenate was centrifuged (10,000 x g, 30 minutes, 4°C) and the inclusion body extraction procedure (Grassick et al. 2004) was conducted on the cell pellet as follows: The pellet was

resuspended in a urea-based inclusion body extraction buffer (20% glycerol, 8 M urea, 50 mM sodium monobasic phosphate, 500 mM sodium chloride, pH 8.0) for 30 minutes at room temperature with gentle shaking. The homogenate was centrifuged (10,000 x g, 30 minutes, 4°C) and the resultant supernatant containing target inclusion body proteins was subsequently utilized for refolding and purification procedures.

Recombinant protein refolding was achieved using slow dialysis as previously described (Grassick et al. 2004). In brief, inclusion body extract was incubated with EDTA (1 mM final concentration) and β -mercaptoethanol (100 mM final concentration) for 2 hours at room temperature with gentle shaking, transferred to dialysis tubing (NMWL: 12,000 – 14,000 Da), and placed for 3 hours into inclusion body exchange buffer (20% glycerol, 8 M urea, 50 mM sodium monobasic phosphate, 500 mM sodium chloride, 1 mM EDTA, pH 8.0) for removal of the β -mercaptoethanol. The buffer was refreshed and dialyzed for an additional 3 hours. The dialysis tubing was then placed into a low-urea refolding buffer (2 M urea, 50 mM sodium monobasic phosphate, 500 mM sodium chloride, 1 mM EDTA, 3 mM reduced glutathione, 0.9 mM oxidized glutathione, pH 8.0) and dialyzed overnight, followed by a no-urea refolding buffer (50 mM sodium monobasic phosphate, 500 mM sodium chloride, 1 mM EDTA, 3 mM reduced glutathione, 0.9 mM oxidized glutathione, pH 8.0) for 36 hours.

Following dialysis, the contents of the tubing were centrifuged to remove insoluble, precipitated proteins (15,000 x g, 15 minutes, 4°C). The supernatant, containing refolded soluble protein, was then exposed to a nickel-nitriloacetic acid (Ni-NTA, 1:1 ratio) slurry (UBPBio, Aurora, CO), packed in a glass frit column (25 x 200 mm, 98 mL volume Kimble-Chase Kontes Flex Column, Vineland, NJ), and allowed to incubate at 4°C for 1 hour on an orbital shaker. Protein purification followed as detailed previously (Morrison et al. 2012). Samples were

concentrated using Amicon Ultra-15 Centrifugal Filter Units (Millipore, NMWL 30 kDa) and protein concentration was determined using a Qubit Fluorimeter (Thermo Scientific) in reference to standard protein concentrations. Protein refolding was checked as activity against PNPX, as described below. An SDS-PAGE gel was run to check protein size and purity, as previously described (Laemmli 1970; Morrison et al. 2012).

Biochemical characterization of Bgxxg1 (Enzyme activity assays).

pH and temperature optima and stability. The pH range and subsequent pH optimum for Bgxxg1 was determined by assaying its β -xylosidase activity (described below) at pH 3, 4, 5, 6, 7, 8, 9, and 10, using the following buffer systems: sodium acetate buffer (pH 3.0-6.0), sodium phosphate buffer (pH 7.0-8.0), and glycine buffer (pH 9.0-10). Similarly, the temperature range and subsequent thermal optimum for Bgxxg1 was determined by assaying its β -xylosidase activity at 25, 30, 39, 50, and 60°C. In a second and separate study, the stability of Bgxxg1 after exposure to pH extremes was determined by assaying its β -xylosidase activity following a one-hour incubation at pH 3, 4, 5, 6, 7, 8, 9, 10, 11, 12, and 13 at 4°C. The following pH buffering systems were used for pH adjustment: sodium acetate buffer (pH 3.0-6.0), sodium phosphate buffer (pH 7.0-8.0), glycine buffer (pH 9.0-10), sodium bicarbonate (pH 11.0), and KCl-NaOH (pH 12-13). Similarly, in a separate study, the thermal stability of Bgxxg1 was determined by assaying its β -xylosidase activity following a one-hour incubation at 4, 25, 30, 37, 39, 50, 60, and 70°C. In all cases, 2.2 μ g of pure Bgxxg1 was used, since this concentration was determined to be optimal in initial testing. Following the one-hour long exposure at the above-described extremes, enzymatic activity was tested at 39°C and pH 6.0, the optimal conditions as determined for this enzyme. All experiments were completed in triplicate, and relative specific activities in relation to the best performing condition (100% activity) were reported.

Enzyme activity assays. All enzyme assays with Bgxl were conducted in pH 6.0 buffer and at 39°C, as these conditions were determined to be optimal for Bgxl. All reagents were purchased from Sigma Aldrich (St. Louis, MO) unless noted otherwise.

Endoglucanase, exoglucanase, xylanase, and mannanase activities were determined using a DNS (3,5-dinitrosalicylic acid)-based assay (Breuil & Saddler 1985), with carboxymethyl cellulose sodium salt (CMC, 1.25% w/v), avicel microcrystalline cellulose (1.25% w/v), beechwood xylan (1.25% w/v), and locust bean gum (0.5% w/v) as substrates, respectively. Glucose, xylose, or mannose were utilized for the generation of a standard curve, dependent on the substrate being tested.

Cellobiohydrolase, β -xylosidase, arabinosidase, mannosidase, β -glucosidase, β -galactosidase, and acetyl xylan esterase activities were determined using (10mM) of the *p*-nitrophenol-based (PNP) substrates: *p*-nitrophenyl- β -D-cellobioside (PNPC), *p*-nitrophenyl- β -D-xylopyranoside (PNPX), *p*-nitrophenyl- β -D-arabinofuranoside (PNPA) *p*-nitrophenyl- β -D-mannoside (PNPM), *p*-nitrophenyl- β -D-glucopyranoside (PNPG), *p*-nitrophenyl- β -D-galactopyranoside (PNPGal), and *p*-nitrophenyl-acetate (PNPAc), respectively (Dashtban et al. 2010; Kubicek 1982; Zhang et al. 2009). Assays were conducted in sodium acetate buffer with sodium carbonate (1M) as a stop reagent. The release of PNP was measured colorimetrically at 420 nm, following the addition of the stop solution. α -glucuronidase activity was assayed using the Megazyme α -glucuronidase assay kit (Wicklow, Ireland).

All experiments were conducted in triplicate. One unit of enzymatic activity (U) was defined as one μ mol of products (reducing sugar equivalents in DNS assays, PNP released in PNP substrate-based assays, and aldouronic acid in α -glucuronidase assay) released from the

substrate per minute. Specific activity was calculated by determining the units released per mg of enzyme.

Enzyme kinetics. Standard procedures were used to determine the K_m , V_{max} , and specific activity of Bgxl on all substrates described above (Lineweaver & Burk 1934). K_m and V_{max} values were obtained using double-reciprocal Lineweaver-Burke plots, which were used to extrapolate from experimentally-derived values using a constant protein concentration (2.2 μ g) and variable PNP-based substrate concentration (0.1 – 100 mM) (Lineweaver & Burk 1934). Given the extinction coefficient of p-nitrophenol (PNP) is 17/mM/cm at 400 nm (Bessey & Love 1952), for a 1 cm path length cuvette and absorbance minimum of 0.010, reliable K_m detection limits in such PNP-based spectrophotometric assays is \approx 500 nM. Therefore, K_m values < 500 nM are referred to as BDL (below detection limit).

Substrate competition assays. Competitive inhibition experiments were conducted to determine whether the observed multiple oligosaccharide hydrolase activities are catalyzed via a single or multiple active sites. In such experiments, the effect of cellobiose (as a competitive inhibitor) on the β -xylosidase activity of Bgxl was measured by conducting the β -xylosidase assay, using 10 mM of PNXP as the substrate, in the presence of different concentrations of cellobiose (0, 10, and 20 mM) and evaluating the impact of cellobiose presence on the release of PNP. Conversely, the effect of xylobiose (as a competitive inhibitor) on the β -glucosidase activity of Bgxl was measured by conducting the β -glucosidase assay (using 10 mM of PNPG as the substrate) in the presence of different concentrations of xylobiose (0, 10, and 20 mM), and evaluating the impact of xylobiose presence on the release of PNP. In both experiments, the effect of inhibitor concentration on K_m and V_{max} was evaluated using Lineweaver-Burke plots (Lineweaver & Burk 1934). All experiments were conducted in triplicate.

Substrate preferences of Bgxl were determined by conducting a substrate competition assay, where Bgxl (2.2 µg of pure enzyme preparation) was challenged by a mixture of xylobiose (10 mM) and cellobiose (10 mM). The kinetics of xylose and glucose release were compared to the results obtained in control experiments where only one substrate (xylobiose or cellobiose) was utilized. Samples were taken at 0, 1, 5, 10, 15, 30, and 60 minutes for the determination of the glucose and xylose concentrations. Glucose was assayed using PGO Enzyme Preparation Capsules (Sigma-Aldrich, St. Louis, MO) and xylose was assayed using Megazyme Xylose Kit (Wicklow, Ireland). All experiments were conducted in triplicate.

Bgxl modeling.

Homology modeling by Iterative Threading ASSEMBly Refinement (I-TASSER) (Roy et al. 2010; Yang et al. 2015; Zhang 2008), was conducted to generate a three-dimensional model of Bgxl using *Thermoanaerobacterium saccharolyticum* β-xylosidase (PDB entry 1UHV) as a template. PyMOL was used to align the Bgxl structural prediction to that of *Thermoanaerobacterium saccharolyticum* (PDB entry 1UHV) to examine and speculate the impact of variations in amino acids residue on the enzyme's active site topology and putative substrate binding capacities (PyMol).

Results

Bgxl phylogenetic affiliation.

Phylogenetic analysis grouped all GH39 sequences into 4 phylogenetically-resolved and bootstrap-supported clades (Classes I-IV in Fig. 1). *Orpinomyces* sp. strain C1A Bgxl protein belonged to Class III, forming a well-supported cluster with GH39 proteins from the anaerobic fungus *Piromyces* sp. strain E2, as well as GH39 proteins from the bacterial genera *Clostridium* and *Teredinibacter* (70-74% sequence identities) (Fig. 1). To our knowledge, none of the GH39

proteins within this specific cluster, or in the entire Class III GH39, has been biochemically characterized.

Physiological characterization.

SDS-PAGE results show that the Bgxxg1 protein is consistent with the predicted size of 42.7 kDa (protein predicted molecular weight is 39.6 KDa + 0.996 kDa linker + 2.101 kDa double histidine tag) (Fig. S3).

The thermal and pH ranges and optima were determined by conducting assays at a range of temperatures and pH's, as described above. Bgxxg1 exhibited activity in a wide range of pH (3-8) and temperatures (25-60°C), with optimal activity at pH 6 and 39°C (Fig. 2A, 2B). The thermal and pH stabilities of Bgxxg1 were examined by conducting activity assays post-stress (pH or thermal)-incubations as described above. Bgxxg1 retained more than 80% of its specific activity post-application of pH stress ranging between 6 and 11 (Fig. 2C), and 60% of its specific activity post application of pH stress of 4, 5, and 12 (Fig. 2C). Further, Bgxxg1 retained $\geq 70\%$ of its specific activity across the broad range of temperature stressors applied (4 – 70°C) (Fig. 2D). In addition, exposure to pH stress from 6-11 and temperature stress from 4-70 °C did not produce results that were significantly different from the optimal conditions (p-value >0.05, 95% confidence interval, Fig. 2).

Substrate specificities and kinetics.

To date, all characterized GH39 enzymes exhibit a narrow substrate range (β -xylosidase or α -L-iduronidase) (Table S1). As predicted by sequence analysis, Bgxxg1 exhibited β -xylosidase activity (11.5 ± 1.2 U/mg, Table 1), strong as compared to previously reported β -xylosidase activities (Table S1). While having a β -xylosidase activity greater than the majority of the field in Table S1, Bgxxg1 does have lower β -xylosidase activity than other anaerobic fungi

317 *Neocallimastix frontalis* (16 U/mg, (Hebraud & Fevre 1990)), *Neocallimastix patriciarum* (30.4
318 U/mg, (Zhu et al. 1994)), *Piromyces communis* (28 U/mg, (Hebraud & Fevre 1988)), and
319 *Sphaeomonas communis* (27 U/mg, (Hebraud & Fevre 1988) (Table 1, S1), however, these are
320 not of the same GH-family. Interestingly, in addition to β -xylosidase activity, Bgxl also
321 exhibited strong β -glucosidase (73.4 ± 7.15 U/mg), β -galactosidase (54.6 ± 2.26 U/mg), and
322 weak xylanase (10.8 ± 1.25 U/mg) activities (Table 1), as compared to reported activities from
323 previously characterized enzymes (Tables S2-S4). Our extensive literature review identified 63
324 enzymes that have been biochemically-characterized to have β -glucosidase activity and, of these,
325 only seven have a reported specific activity higher than that of Bgxl (Table S2), including
326 *Candida peltata* (108 U/mg, (Saha & Bothast 1996)), *Thermoascus aurantiacus* (232 U/mg,
327 (Tong et al. 1980)), and *Trichoderma reesei* (768 U/mg, (Takashima et al. 1998)). Similarly, we
328 only identified three β -galactosidase with a reported higher activity than Bgxl (Table S3),
329 including *Alicyclobacillus acidocaldarius* (229 U/mg, (Yuan et al. 2008)), *Bifidobacterium*
330 *adolescentis* (526 U/mg, (Hinz et al. 2004)), and *Thermus aquaticus* (1750 U/mg, (Ulrich et al.
331 1972)). On the other hand, the xylanase activity of Bgxl is relatively weak, with many
332 previously reported xylanases exhibiting a much higher specific activity (Table S4), such as
333 *Aspergillus niger* (19 U/mg, 25 U/mg, 35 U/mg, and 48 U/mg, (John et al. 1979)) and
334 *Trichoderma reesei* (46 U/mg, (Takashima et al. 1998)). Bgxl exhibited no detectable
335 exoglucanase, endoglucanase, mannanase, arabinosidase, acetyl xylan esterase,
336 cellobiohydrolase, mannosidase, or α -glucuronidase activities.

337 In addition to its high β -xylosidase, β -glucosidase, and β -galactosidase specific activities,
338 Bgxl exhibited remarkably high affinities towards all examined substrates, with K_m values

(calculated via extrapolation through Lineweaver-Burke plot) in the low nM range for PNPG and PNPGal, the low μ M range for PNPX (Table 2, Table S1-S4).

Substrate competition studies.

Substrate competition studies were conducted using a variable concentration of an unlabeled substrate (acting as an inhibitor) and a fixed concentration of a chromophore (PNP-based) substrate (Table 3). The results strongly suggest the occurrence of cross-substrate competitive inhibition between xylobiose and cellobiose (Table 3), since the presence of increasing concentrations of a single substrate lowers the specific activity and increases the K_m of the enzyme towards the other substrate, whilst not affecting its V_{max} (K_m and V_{max} calculated via extrapolation through Lineweaver-Burke plot). This pattern strongly indicates that a single active site is responsible for the observed activities (Table 3), a conclusion that is in agreement with the lack of identifiable additional domains other than pfam01229 in Bgxxg1, as well as with the structural modeling data described below.

In single substrate assays, Bgxxg1 was capable of converting cellobiose to glucose and xylobiose to xylose at a very fast rate (Fig. 3A, 3B). This reaction occurs more quickly for xylobiose, as a stable maximal xylose concentration is reached after only 1 minute of incubation (Fig. 3B), compared to 15 minutes for glucose release from cellobiose (Fig. 3A). However, the extent of sugar release at the conclusion of the experiment was higher in cellobiose incubations (Fig. 3A) than xylobiose incubations (Fig. 3B). Competition studies using equimolar concentrations of both substrates revealed the preference of Bgxxg1 for xylobiose, since a higher proportion of xylose rather than glucose was detected within the first 15 minutes of the incubation (Fig. 3C). Nevertheless, the final concentrations of sugars released after 60 minutes of incubation did not differ when comparing single substrate versus competition experiments (Fig.

3A-3C). Similar to the patterns observed in single substrate assays, Bgxxg1 reduced a larger amount of cellobiose to glucose than xylobiose to xylose in competition experiments (Fig. 3C), which is consistent with the higher affinity (lower K_m value) of Bgxxg1 for PNPG (12.5 nM) over PNPX (4.85 μ M) (Table 2).

Structure activity predictions.

The Bgxxg1 protein sequence was submitted to I-TASSER for structural prediction by Iterative Threading ASSEmbly Refinement (Roy et al. 2010; Yang et al. 2015; Zhang 2008) utilizing the β -xylosidase originating from *Thermoanaerobacterium saccharolyticum* (PDB entry 1UHV) as a template for model creation (Roy et al. 2010; Yang et al. 2004; Yang et al. 2015; Zhang 2008). Bgxxg1 is predicted to have three distinct domains: a catalytic $(\alpha/\beta)_8$ barrel fold domain (position 26-307), a small α -helical domain (position 1-25), and a β sandwich domain (position 308-344) (Fig. S4). Overall, the structure is predicted to contain 11 β -sheets (8 in $(\alpha/\beta)_8$ -barrel, 3 in β -sandwich), and 10 α -helices (8 in $(\alpha/\beta)_8$ -barrel, 2 in α -domain). The catalytic $(\alpha/\beta)_8$ -barrel fold domain is predicted to consist of eight parallel β -sheets (β 1- β 8), and eight parallel α -helices (α 1- α 8). Consistent with β -xylosidases of *Thermoanaerobacterium saccharolyticum* (1UHV) and *Geobacillus stearothermophilus* (1PX8), the active site pocket of Bgxxg1 is predicted to be located on the upper side of the $(\alpha/\beta)_8$ -barrel (Czjzek et al. 2005; Yang et al. 2004) (Fig. S4). Alignment and structural predictions identified the conservation of the general acid-base active site residue Glu127 in the C-terminal of β 3, as part of the GH39-conserved Asn126-Glu127-Pro128 motif as well as the nucleophilic residue Glu225 in β 6 (Fig. 4) (Czjzek et al. 2005; Yang et al. 2004).

Using the predicted model we sought to infer structural differences potentially responsible for the observed relaxed substrate specificities in Bgxxg1 by investigating the amino

acid conservation patterns between Bgxxg1 and all structurally and/or biochemically-
characterized β -xylosidases. These enzymes are: *Thermoanaerobacterium saccharolyticum* β -
xylosidase (Yang et al. 2004), *Geobacillus stearothermophilus* β -xylosidase (Bhalla et al. 2014;
Czjzek et al. 2005), and *Bacillus halodurans* C-125 protein BH1068 (Wagschal et al. 2008), all
of which belong to Class II (Fig. 1), as well as *Caulobacter crescentus* CcXynB2 (Correa et al.
2012), which belongs to Class I (Fig. 1). All of these enzymes have previously been reported to
possess β -xylosidase activity (Bhalla et al. 2014; Correa et al. 2012; Czjzek et al. 2005;
Wagschal et al. 2008; Yang et al. 2004). We focused on 25 amino acids in two groups: (i) those
previously shown to be important for β -xylosidase activity (Czjzek et al. 2005; Yang et al. 2004)
[this group includes (in addition to the conserved general acid-base and nucleophilic active sites
described above) amino acids providing the tight hydrogen bonding necessary to stabilize the
xylosyl-enzyme intermediate formed during the reaction, such as Arg52, His54, Asn159, His228,
Tyr230, Glu278, Trp315, Glu322, and Glu323 (locations refer to position in 1UHV)], as well as
(ii) those physically interacting with the active site as deduced by the predicted Bgxxg1 model
(Fig. S3A) [this group includes Val46, Val81, Ile124, Trp125, Gly130, Thr131, Trp132, Phe139,
Pro162, Cys163, Tyr164, Ser165, Lys171, His192, Asn242, and Lys247 (locations refer to
position in Bgxxg1)]. Of these 25 amino acids, 15 differed between Bgxxg1 and the four other
proteins. Five of these 15 amino acids were not conserved amongst any of the five sequences
studied and so were not further investigated (Fig. 4). Therefore, 10 distinct differences (8
substitutions and 2 deletions) between Bgxxg1 on one hand and the four biochemically-
characterized β -xylosidases on the other were identified (Table 4). These differences that are
predicted to exist in or around the active site of Bgxxg1 would putatively impact the size, charge,
and/or polarity within the active site (Table 4, Fig. S4).

The expanded substrate specificity observed in this study could be a unique trait in Bgxl, or it could be specific to all GH39 CAZymes of anaerobic fungi (e.g. Class III-C), or to the entire Class III β -xylosidases. Based on the above speculations about the amino acids potentially responsible for Bgxl relaxed specificity, we further investigated the conservation of these 10 amino acid changes (Table 4) within class III of GH39 proteins. Bgxl (as well as other GH39 proteins encoded in C1A genome), all three GH39 proteins from the *Piromyces* genome (accession numbers shown in Fig. 1), and all additional sequences from Class III-C belonging to the genera *Clostridium* and *Teredinibacter* were found to encode 9 of the 10 observed amino acid substitutions (Table 4). However, within the broader Class III, little similarity in key amino acids was observed between Bgxl sequences and β -xylosidases belonging to Class III-A, III-B, or III-D (Table 4). Collectively, these results putatively suggest that the observed relaxed specificity in Bgxl could be exclusive to Class III-C β -xylosidases.

Discussion

In this study, we used a transcriptomics-guided approach to identify, clone, express, and characterize a GH39 protein (Bgxl) from the anaerobic gut fungus *Orpinomyces* sp. strain C1A. Our results demonstrate that the expressed protein is multifunctional, possessing strong β -xylosidase (11.5 U/mg), β -glucosidase (73.4 U/mg), and β -galactosidase (54.6 U/mg) activities, as well as a weak xylanase activity (10.8 U/mg) (Table 1, 2), as compared to previously characterized enzymes (Tables S1-S4). This novel multi-functionality has not been previously reported in GH39 enzymes (Bhalla et al. 2014), and therefore this work expands on the known activities of GH39 CAZyme family. Further, Bgxl retains high levels of activity over a wide range of temperatures (>80% of activity retained between 4-70°C) (Fig. 2D) and pH values (>80% of activity retained between pH 6-11) (Fig. 2C). Though the composition of commercial

enzymes cocktails are largely proprietary, the presence of 80-200 different components within a mixture has been previously reported (Banerjee et al. 2010; Van Dyk & Pletschke 2012). It is intuitive to think that the inclusion of such a large number of enzymes represents a large contribution to the cost of production. It is here that Bgxxg1 would be beneficial, as the inclusion of a single enzyme, possessing multiple strong activities, would lower the cost of production in biorefineries and therefore would be beneficial to the bottom line.

In addition to its relaxed substrate specificity, the enzyme displays strong kinetic properties (high specific activity and affinity) towards its multiple substrates (K_m and V_{max} values calculated via extrapolation through Lineweaver-Burke plot). As a β -xylosidase, Bgxxg1 has one of the highest β -xylosidase specific activity among all reported ambient ($<50^\circ\text{C}$) β -xylosidases, but lower than other anaerobic fungi *Neocallimastix frontalis* (16 U/mg, (Hebraud & Fevre 1990)), *Neocallimastix patriciarum* (30.4 U/mg, (Zhu et al. 1994)), *Piromyces communis* (28 U/mg, (Hebraud & Fevre 1988)), and *Sphaeomonas communis* (27 U/mg, (Hebraud & Fevre 1988) (Table 1, S1). Bgxxg1 also one of the highest specific activities amongst known GH39 β -xylosidases (Tables 1, S1), with a lower specific activity than the thermophilic *Thermoanaerobacterium saccharolyticum* (53.8 U/mg, (Shao et al. 2011)) and the thermophilic *Geobacillus stearothermophilus* (133 U/mg, (Bhalla et al. 2014)). Compared to other characterized β -glucosidases, Bgxxg1 has the highest specific activity for all ambient temperature β -glucosidases, and one of the highest reported specific activities among all β -glucosidase (members of GH1, GH3, GH5, GH9, and GH30 (Cairns & Esen 2010)), regardless of optimal temperature and GH affiliation (Tables 1, S2). Finally, compared to other characterized β -galactosidases, Bgxxg1 has the highest specific activity for all ambient temperature β -galactosidases, and one of the highest reported specific activities among all β -galactosidases

(members of GH1, GH2, GH35, and GH42 (Skalova et al. 2005)) regardless of optimal temperature and GH affiliation (Tables 1, 2, S4).

We reason that the observed kinetics and substrate specificity of Bg_{xg}1 are beneficial for strain C1A and are highly desirable for a saccharolytic enzyme acting within the highly competitive rumen environment, where strain C1A originally existed (*Orpinomyces* sp. strain C1A was isolated from the feces of an angus steer (Youssef et al. 2013)). The high specific activity and high substrate affinity may aid in fast and efficient scavenging of sugars from the surrounding environment, where competition for sugars/oligosaccharide produced by saccharolytic enzymes are intense, and where free sugar levels are permanently low (Garcia-Vallve et al. 2000). We hence speculate that the survival in an anaerobic, eutrophic, and highly competitive environment might be responsible for the acquisition, retention and directed evolution of anaerobic fungal β -xylosidases towards superior kinetics and relaxed specificities.

Sequence analysis and structural predictive modeling (Figs. 4 and S4), and substrate competition experiments (Table 3) predict the presence of a single conserved active site within the $(\alpha/\beta)_8$ -barrel fold structure typically observed in GH39-family enzymes (Czjzek et al. 2005; Yang et al. 2004) (with the conserved catalytic nucleophile (Glu225) and general acid-base residue (Glu127)) and potentially mediating all observed hydrolytic activities). To provide clues regarding the structural basis of the observed multi-functionality, comparison of amino acid conservation patterns putatively affecting the active site topology between Bg_{xg}1 and biochemically characterized GH39 xylosidases, all four of which display no additional activities beyond β -xylosidase, was undertaken. We identified ten different distinct amino acid changes (8 substitutions and 2 deletions) (Table 4, Figs. S4 and 5) in Bg_{xg}1 that putatively affect the polarity (Tyr vs. Val46, Phe vs. Thr131, Tyr vs. Phe139, Ala vs. Cys163, Trp vs. Lys171, Tyr vs.

477 Leu194, and Ala vs. Arg242), constitute significant size changes (Tyr vs. Val46, Phe vs. Thr131,
 478 Tyr vs. Leu194, and Ala vs. Arg242), result in the addition of charged moieties or unique
 479 functional groups (Asn vs. Asp129, Ala vs. Cys163, Trp vs. Lys171, and Ala vs. Arg242), or
 480 result in the deletion of a negatively charged residue, previously determined to be important
 481 (Glu322-323 vs. deletion) to the active site (Czjzek et al. 2005). The impact of these speculated
 482 changes is unclear, and it remains to be seen if any, all, or a combination of the above differences
 483 is responsible for the observed relaxed specificity. However, while all these amino acid changes
 484 are speculated to theoretically explain the relaxed specificity of Bgxl, one such difference is
 485 peculiar and deserves special scrutiny; deletions/gaps in the Bgxl sequence as opposed to
 486 negatively charged glutamic acids in the other four sequences (Table 4, Fig. S4S). GH39
 487 enzymes belong to the wider family of β -1,4-retaining hydrolases of clan GH-A e.g. GH1 β -
 488 glucosidase and GH5 cellulases. Differences in structure between β 1,4-glucose cleaving
 489 enzymes and β 1,4-xylose cleaving enzymes within clan GH-A have been extensively
 490 investigated (Czjzek et al. 2005; Czjzek et al. 2001; Ducros et al. 1995; Hovel et al. 2003;
 491 Verdoucq et al. 2004). Such studies have demonstrated that, within the active site of β 1,4-
 492 glucose cleaving enzymes, a Gln residue (corresponding to position 39 in the enzyme dhurinase
 493 of *Sorghum bicolor* (Czjzek et al. 2005; Ducros et al. 1995; Verdoucq et al. 2004)) interacts with
 494 the substrate by forming a hydrogen bond with O3 and O4 of the glucose moiety (Czjzek et al.
 495 2005; Ducros et al. 1995). On the other hand, β 1,4-xylosidases acting on C5 sugar dimers
 496 contain a Glu residue in lieu of Gln (at position 322-323 in *Thermoanaerobacterium*
 497 *saccharolyticum*, Fig. 4 and S4, Table 4) that binds to O3 and O4 of the xylose moiety (Czjzek et
 498 al. 2005). Interestingly, these Glu residues are aligned with a gap in the sequence of the
 499 multifunctional Bgxl (Fig. 4), with no apparent occurrence of either Glu or Gln amino acids

within the vicinity. Structurally predictive modeling suggests that in lieu of these Glu322-323 residues (1UHV numbering) Bgxxg1 is predicted to possess Gly-Arg at an approximately sterically-similar location near the active site (Figure S4R-S), representing a significant change from two negatively-charged residues, to an uncharged and positively-charged pair of residues. Since the Glu residues in biochemically characterized β -xylosidases are shown to be important for stabilizing intermediates (Czjzek et al. 2005), the predicted absence of these residues in Bgxxg1 and their speculated replacement with Gly-Arg suggests that Bgxxg1 might employ a different mechanism for stabilizing its intermediates during the catalytic process; however, this speculation will require further investigation.

The ecological relevance, global distribution, and evolutionary patterns of multi-functionality within GH39 β -xylosidases remain to be conclusively determined. Phylogenetic analysis demonstrated the occurrence of nine out of ten amino acids substitutions/deletions in all sequenced members of Class III-C, residues which we speculate to be of importance to the observed multi-functionality of Bgxxg1, but as Bgxxg1 is the only biochemically-characterized enzyme within Class III, this analysis is purely speculative (Table 4, alignment in Fig. S5). In addition to anaerobic fungal sequences, Class III-C β -xylosidases contain sequences from the genera *Clostridium* and *Teredinibacter* (Fig. 1). Since it has been previously demonstrated that the xylanolytic machinery in anaerobic fungi, including β -xylosidases, has been acquired from bacteria via horizontal gene transfer (Youssef et al. 2013), and speculating that some or all of the amino acids substitutions/deletions in members of class III-C collectively account for the observed multi-functionality (though it is unknown, at this time, whether these GH39 enzymes possess this multi-functionality), therefore we reason that the observed distribution pattern suggests the evolution of relaxed specificity in GH39 β -xylosidases within the domain Bacteria,

prior to the acquisition of GH39 β -xylosidases by the anaerobic fungi and that the acquired capability is speculated to be retained in all anaerobic fungal GH39 β -xylosidases.

Conclusions

In conclusion, we have characterized a novel β -xylosidase that represents the first GH39-family enzyme cloned and expressed from anaerobic fungi. The enzyme is multi-functional, capable of hydrolyzing cellobiose, xylobiose, as well as several PNP-glycosides. It also displays high affinity towards various substrates, retains activity over a wide range of temperatures and pHs, and possesses excellent temperature and thermal stability. Structurally predictive modeling identified putative differences which potentially could account for the observed relaxed specificity. Collectively, these capabilities render Bg_{xg}1 an excellent candidate for inclusion in enzyme cocktails mediating cellulose and hemicellulose saccharification from lignocellulosic biomass (Morrison et al. 2016).

Acknowledgements

We thank Dr. Gilbert John (Oklahoma State University) for supplying the *E. coli* BL21(DE3)pLysS cells used in this study. We also thank Dr. Robert Gruninger for helpful discussions.

References

- Banerjee G, Scott-Craig JS, and Walton JD. 2010. Improving Enzymes for Biomass Conversion: A Basic Research Perspective. *Bioenergy Research* 3:82-92. 10.1007/s12155-009-9067-5
- Bessey OA, and Love RH. 1952. Preparation and measurement of the purity of the phosphatase reagent, disodium para-nitrophenyl phosphate. *J Biol Chem* 196:175-178.
- Bhalla A, Bischoff KM, and Sani RK. 2014. Highly thermostable GH39 beta-xylosidase from a *Geobacillus* sp strain WSUCF1. *BMC Biotechnol* 14:963-973. Artn 963 10.1186/S12896-014-0106-8
- Borneman WS, Akin DE, and Ljungdahl LG. 1989. Fermentation products and plant-cell wall-degrading enzymes produced by monocentric and polycentric anaerobic ruminal fungi. *Appl Environ Microbiol* 55:1066-1073.
- Brennan Y, Callen WN, Christoffersen L, Dupree P, Goubet F, Healey S, Hernandez M, Keller M, Li K, Palackal N, Sittenfeld A, Tamayo G, Wells S, Hazlewood GP, Mathur EJ, Short JM, Robertson DE, and Steer BA. 2004. Unusual microbial xylanases from insect guts. *Appl Environ Microbiol* 70:3609-3617. Doi 10.1128/Aem.70.6.3609-3617.2004
- Breuil C, and Saddler JN. 1985. Comparison of the 3,5-dinitrosalicylic acid and Nelson-Somogyi methods of assaying for reducing sugars and determining cellulase activity. *Enzyme Microb Tech* 7:327-332. Doi 10.1016/0141-0229(85)90111-5
- Bronnenmeier K, and Staudenbauer WL. 1988. Purification and properties of an extracellular beta-glucosidase from the cellulolytic thermophile *Clostridium stercorarium*. *Appl Microbiol Biot* 28:380-386.
- Cairns JRK, and Esen A. 2010. Beta-glucosidases. *Cell Mol Life Sci* 67:3389-3405. 10.1007/s00018-010-0399-2

Correa JM, Graciano L, Abrahao J, Loth EA, Gandra RF, Kadowaki MK, Henn C, and Simao
RDG. 2012. Expression and characterization of a GH39 beta-xylosidase II from
Caulobacter crescentus. *Appl Biochem Biotech* 168:2218-2229. 10.1007/s12010-012-
9931-1

Couger MB, Youssef NH, Struchtemeyer CG, Liggenstoffer AS, and Elshahed MS. 2015.
Transcriptomics analysis of lignocellulosic biomass degradation by the anaerobic fungal
isolate *Orpinomyces* sp. strain C1A. *Biotechnol Biofuels* 8:208-224.

Czjzek M, Ben David A, Braman T, Shoham G, Henrissat B, and Shoham Y. 2005. Enzyme-
substrate complex structures of a GH39 beta-xylosidase from *Geobacillus*
stearothermophilus. *J Mol Biol* 353:838-846. 10.1016/j.jmb.2005.09.003

Czjzek M, Cicek M, Zamboni V, Burmeister WP, Bevan DR, Henrissat B, and Esen A. 2001.
Crystal structure of a monocotyledon (maize ZMGlu1) beta-glucosidase and a model of
its complex with p-nitrophenyl beta-D-thioglucoside. *Biochem J* 354:37-46. Doi
10.1042/0264-6021:3540037

Dashtban M, Maki M, Leung KT, Mao CQ, and Qin WS. 2010. Cellulase activities in biomass
conversion: measurement methods and comparison. *Crit Rev Biotechnol* 30:302-309.
10.3109/07388551.2010.490938

Ducros V, Czjzek M, Belaich A, Gaudin C, Fierobe HP, Belaich LP, Davies GJ, and Haser R.
1995. Crystal structure of the catalytic domain of a bacterial cellulase belonging to family
5. *Structure* 3:939-949. Doi 10.1016/S0969-2126(01)00228-3

Elshahed MS. 2010. Microbiological aspects of biofuel production: current status and future
directions. *J Adv Res* 1:103-111.

585 Garcia-Vallve S, Romeu A, and Palau J. 2000. Horizontal gene transfer of glycosyl hydrolases of
586 the rumen fungi. *Mol Biol Evol* 17:352-361.

587 Grassick A, Murray PG, Thompson R, Collins CM, Byrnes L, Birrane G, Higgins TM, and
588 Tuohy MG. 2004. Three-dimensional structure of a thermostable native
589 cellobiohydrolase, CBHIB, and molecular characterization of the cel7 gene from the
590 filamentous fungus, *Talaromyces emersonii*. *Eur J Biochem* 271:4495-4506.
591 10.1111/j.1432-1033.2004.04409.x

592 Harhangi HR, Freelove AC, Ubhayasekera W, van Dinther M, Steenbakkens PJ, Akhmanova A,
593 van der Drift C, Jetten MS, Mowbray SL, Gilbert HJ, and Op den Camp HJ. 2003.
594 Cel6A, a major exoglucanase from the cellulosome of the anaerobic fungi *Piromyces* sp.
595 E2 and *Piromyces equi*. *Biochim Biophys Acta* 1628:30-39.

596 Hebraud M, and Fevre M. 1988. Characterization of glycoside and polysaccharide hydrolases
597 secreted by the rumen anaerobic fungi *Neocallimastix frontalis*, *Sphaeromonas communis*
598 and *Piromonas communis*. *J Gen Microbiol* 134:1123-1129.

599 Hebraud M, and Fevre M. 1990. Purification and characterization of an extracellular beta-
600 xylosidase from the rumen anaerobic fungus *Neocallimastix frontalis*. *FEMS Microbiol*
601 *Lett* 72:11-16. DOI 10.1111/j.1574-6968.1990.tb03853.x

602 Hess M, Sczyrba A, Egan R, Kim TW, Chokhawala H, Schroth G, Luo SJ, Clark DS, Chen F,
603 Zhang T, Mackie RI, Pennacchio LA, Tringe SG, Visel A, Woyke T, Wang Z, and Rubin
604 EM. 2011. Metagenomic discovery of biomass-degrading genes and genomes from cow
605 rumen. *Science* 331:463-467. 10.1126/science.1200387

606 Hill J, Nelson E, Tilman D, Polasky S, and Tiffany D. 2006. Environmental, economic, and
 607 energetic costs and benefits of biodiesel and ethanol biofuels. *P Natl Acad Sci USA*
 608 103:11206-11210. 10.1073/pnas.0604600103

609 Hinz SWA, van den Broek LAM, Beldman G, Vincken JP, and Voragen AGJ. 2004. Beta-
 610 galactosidase from *Bifidobacterium adolescentis* DSM20083 prefers beta(1,4)-
 611 galactosides over lactose. *Appl Microbiol Biot* 66:276-284. 10.1007/s00253-004-1745-9

612 Hovel K, Shallom D, Niefind K, Belakhov V, Shoham G, Baasov T, Shoham Y, and Schomburg
 613 D. 2003. Crystal structure and snapshots along the reaction pathway of a family 51 alpha-
 614 L-arabinofuranosidase. *EMBO J* 22:4922-4932. Doi 10.1093/Emboj/Cdg494

615 John M, Schmidt B, and Schmidt J. 1979. Purification and some properties of five endo-1,4-beta-
 616 D-xylanases and a beta-D-xylosidase produced by a strain of *Aspergillus niger*. *Can J*
 617 *Biochem Cell B* 57:125-134.

618 Kubicek CP. 1982. Beta-glucosidase excretion by *Trichoderma pseudokoningii* - correlation with
 619 cell-wall bound beta-1.3-glucanase activities. *Arch Microbiol* 132:349-354. Doi
 620 10.1007/Bf00413388

621 Kumar R, Singh S, and Singh OV. 2008. Bioconversion of lignocellulosic biomass: biochemical
 622 and molecular perspectives. *J Ind Microbiol Biot* 35:377-391. 10.1007/s10295-008-0327-
 623 8

624 Kumar S, and Ramon D. 1996. Purification and regulation of the synthesis of a beta-xylosidase
 625 from *Aspergillus nidulans*. *FEMS Microbiol Lett* 135:287-293. DOI 10.1111/j.1574-
 626 6968.1996.tb08003.x

627 Laemmli UK. 1970. Cleavage of Structural Proteins during Assembly of Head of Bacteriophage-
 628 T4. *Nature* 227:680-&. Doi 10.1038/227680a0

- 629 Ligenstoffer AS, Youssef NH, Wilkins MR, and Elshahed MS. 2014. Evaluating the utility of
630 hydrothermolysis pretreatment approaches in enhancing lignocellulosic biomass
631 degradation by the anaerobic fungus *Orpinomyces* sp. strain C1A. *J Microbiol Meth*
632 104:43-48. 10.1016/j.mimet.2014.06.010
- 633 Lineweaver H, and Burk D. 1934. The determination of enzyme dissociation constants. *J Am*
634 *Chem Soc* 56:658-666. Doi 10.1021/Ja01318a036
- 635 Liu ZL, Saha BC, and Slininger PJ. 2008. Lignocellulosic biomass conversion to ethanol by
636 *Saccharomyces*. In: Harwood CS, Demain AL, and Wall JD, eds. *Bioenergy*. Washington
637 D.C.: ASM Press.
- 638 Ljungdahl LG. 2008. The cellulase/hemicellulase system of the anaerobic fungus *Orpinomyces*
639 PC-2 and aspects of its applied use. *Ann Ny Acad Sci* 1125:308-321.
640 10.1196/annals.1419.030
- 641 Lombard V, Ramulu HG, Drula E, Coutinho PM, and Henrissat B. 2014. The carbohydrate-
642 active enzymes database (CAZy) in 2013. *Nucleic Acids Res* 42:D490-D495.
643 10.1093/nar/gkt1178
- 644 Matsuo M, and Yasui T. 1984. Purification and some properties of beta-xylosidase from
645 *Trichoderma viride*. *Agr Biol Chem* 48:1845-1852.
- 646 Morrison JM, Elshahed MS, and Youssef NH. 2016. A defined enzyme cocktail from the
647 anaerobic fungus *Orpinomyces* sp. strain C1A effectively releases sugars from pretreated
648 corn stover and switchgrass. *Sci Rep* Accepted.
- 649 Morrison JM, Wright CM, and John GH. 2012. Identification, isolation and characterization of a
650 novel azoreductase from *Clostridium perfringens*. *Anaerobe* 18:229-234.
651 10.1016/j.anaerobe.2011.12.006

652 National Research Council N. 2011. Renewable Fuel Standard: Potential Economic and
653 Environmental Effects of U.S. Biofuel Policy. Washington, D.C.

654 PyMol. The PyMOL Molecular Graphics System. Version 1.7.4 ed: Schrodinger, LLC.

655 Ragauskas AJ, Williams CK, Davison BH, Britovsek G, Cairney J, Eckert CA, Frederick WJ,
656 Hallett JP, Leak DJ, Liotta CL, Mielenz JR, Murphy R, Templer R, and Tschaplinski T.
657 2006. The path forward for biofuels and biomaterials. *Science* 311:484-489.
658 10.1126/science.1114736

659 Roy A, Kucukural A, and Zhang Y. 2010. I-TASSER: a unified platform for automated protein
660 structure and function prediction. *Nat Protoc* 5:725-738. 10.1038/nprot.2010.5

661 Saha BC, and Bothast RJ. 1996. Production, purification, and characterization of a highly
662 glucose-tolerant novel beta-glucosidase from *Candida peltata*. *Appl Environ Microbiol*
663 62:3165-3170.

664 Scheller HV, and Ulvskov P. 2010. Hemicelluloses. *Annu Rev Plant Biol* 61:263-289.
665 10.1146/annurev-arplant-042809-112315

666 Shao WL, Xue YM, Wu AL, Kataeva I, Pei JJ, Wu HW, and Wiegel J. 2011. Characterization of
667 a bovel beta-xylosidase, XylC, from *Thermoanaerobacterium saccharolyticum* JW/SL-
668 YS485. *Appl Environ Microbiol* 77:719-726. 10.1128/Aem.01511-10

669 Sievers F, Wilm A, Dineen D, Gibson TJ, Karplus K, Li WZ, Lopez R, McWilliam H, Remmert
670 M, Soding J, Thompson JD, and Higgins DG. 2011. Fast, scalable generation of high-
671 quality protein multiple sequence alignments using Clustal Omega. *Mol Syst Biol* 7:1-6.
672 Artin 539 10.1038/Msb.2011.75

673 Skalova T, Dohnalek J, Spiwok V, Lipovova P, Vondrackova E, Petrokova H, Duskova J, Strnad
674 H, Kralova B, and Hasek J. 2005. Cold-active beta-galactosidase from *Arthrobacter* sp

675 C2-2 forms compact 660 kDa hexamers: crystal structure at 1.9 angstrom resolution. *J*
676 *Mol Biol* 353:282-294. 10.1016/j.jmb.2005.08.028

677 Stamatakis A. 2014. RAxML version 8: a tool for phylogenetic analysis and post-analysis of
678 large phylogenies. *Bioinformatics* 30:1312-1313. 10.1093/bioinformatics/btu033

679 Takashima S, Iikura H, Nakamura A, Hidaka M, Masaki H, and Uozumi T. 1998.
680 Overproduction of recombinant *Trichoderma reesei* cellulases by *Aspergillus oryzae* and
681 their enzymatic properties. *J Biotechnol* 65:163-171. Doi 10.1016/S0168-1656(98)00084-
682 4

683 Tamura K, Stecher G, Peterson D, Filipinski A, and Kumar S. 2013. MEGA6: molecular
684 evolutionary genetics analysis version 6.0. *Mol Biol Evol* 30:2725-2729.
685 10.1093/molbev/mst197

686 Tong CC, Cole AL, and Shepherd MG. 1980. Purification and properties of the cellulases from
687 the thermophilic fungus *Thermoascus aurantiacus*. *Biochem J* 191:83-94.

688 Ulrich JT, Temple KL, and Mcfeters GA. 1972. Induction and characterization of beta-
689 galactosidase in an extreme thermophile. *J Bacteriol* 110:691-698.

690 Van Dyk JS, and Pletschke BI. 2012. A review of lignocellulose bioconversion using enzymatic
691 hydrolysis and synergistic cooperation between enzymes-Factors affecting enzymes,
692 conversion and synergy. *Biotechnol Adv* 30:1458-1480.
693 10.1016/j.biotechadv.2012.03.002

694 vanPeij NNME, Brinkmann J, Vrsanska M, Visser J, and deGraaff LH. 1997. Beta-xylosidase
695 activity, encoded by xlnD, is essential for complete hydrolysis of xylan by *Aspergillus*
696 *niger* but not for induction of the xylanolytic enzyme spectrum. *Eur J Biochem* 245:164-
697 173.

698 Verdoucq L, Moriniere J, Bevan DR, Esen A, Vasella A, Henrissat B, and Czjzek M. 2004.
699 Structural determinants of substrate specificity in family 1 beta-glucosidases - Novel
700 insights from the crystal structure of sorghum dhurrinase-1, a plant beta-glucosidase with
701 strict specificity, in complex with its natural substrate. *J Biol Chem* 279:31796-31803.
702 10.1074/jbc.M402918200

703 Wagschal K, Franqui-Espiet D, Lee CC, Robertson GH, and Wong DWS. 2008. Cloning,
704 expression and characterization of a glycoside hydrolase family 39 xylosidase from
705 *Bacillus halodurans* C-125. *Appl Biochem Biotech* 146:69-78. 10.1007/s12010-007-
706 8055-5

707 Wang HC, Chen YC, Huang CT, and Hseu RS. 2013. Cloning and characterization of a
708 thermostable and pH-stable cellobiohydrolase from *Neocallimastix patriciarum* J11.
709 *Protein Expres Purif* 90:153-159. 10.1016/j.pep.2013.06.004

710 Yang JK, Yoon HJ, Ahn HJ, Lee BI, Pedelacq JD, Liong EC, Berendzen J, Laivenieks M, Vieille
711 C, Zeikus GJ, Vocadlo DJ, Withers SG, and Suh SW. 2004. Crystal structure of beta-D-
712 xylosidase from *Thermoanaerobacterium saccharolyticum*, a family 39 glycoside
713 hydrolase. *J Mol Biol* 335:155-165. 10.1016/j.jmb.2003.10.026

714 Yang JY, Yan RX, Roy A, Xu D, Poisson J, and Zhang Y. 2015. The I-TASSER Suite: protein
715 structure and function prediction. *Nat Methods* 12:7-8. 10.1038/nmeth.3213

716 Youssef NH, Couger MB, Struchtemeyer CG, Ligginstoffer AS, Prade RA, Najar FZ, Atiyeh
717 HK, Wilkins MR, and Elshahed MS. 2013. The genome of the anaerobic fungus
718 *Orpinomyces* sp strain C1A reveals the unique evolutionary history of a remarkable plant
719 biomass degrader. *Appl Environ Microbiol* 79:4620-4634. 10.1128/Aem.00821-13

Yuan TZ, Yang PL, Wang YR, Meng K, Luo HY, Zhang W, Wu NF, Fan YL, and Yao B. 2008. Heterologous expression of a gene encoding a thermostable beta-galactosidase from *Alicyclobacillus acidocaldarius*. *Biotechnol Lett* 30:343-348. 10.1007/s10529-007-9551-y

Zhang Y. 2008. I-TASSER server for protein 3D structure prediction. *BMC Bioinformatics* 9:40-48. Artid 40 10.1186/1471-2105-9-40

Zhang YHP, Hong J, and Xinhao Y. 2009. Cellulase Assays. In: Mielenz JR, ed. *Biofuels: Methods and Protocols*: Humana Press, 213-231.

Zhu H, Cheng KJ, and Forsberg CW. 1994. A truncated beta-xylosidase from the anaerobifungus *Neocallimastix patriciarum* 27. *Can J Microbiol* 40:484-490.

Figure Legends

Figure 1. Phylogenetic analysis of GH39 β -xylosidases, including Bgxl. Sequences annotated as GH39 β -xylosidases (n=200 sequences, October 28, 2015) were retrieved from CAZyme databases (Lombard et al. 2014). Genbank accession numbers are shown for reference proteins (due to the unavailability of *Piromyces* proteins in Genbank, those proteins are shown as JGI accession numbers). The Maximum Likelihood tree was generated in RAxML (Stamatakis 2014) using a BLOSUM62 substitution matrix and a GAMMA model of rate heterogeneity. The model estimated an alpha parameter of 2.069. Bootstraps values (100 replicates) are shown for nodes with >50 bootstrap support. The sequences were empirically classified into four classes (Classes I-IV), and Class III, to which Bgxl is affiliated, is further classified into four distinct lineages (III-A-III-D). The α -iduronidase sequence from *Mus musculus* was utilized as an outgroup. β -xylosidases that were previously characterized biochemically were phylogenetically affiliated with either Class II (*Bacillus halodurans* (BAB04787.1) and *Geobacillus stearothermophilus* (ABI49941.1) in bottom Firmicutes wedge, and *Thermoanaerobacterium saccharolyticum* (AAB68820.1) in middle Firmicutes wedge) or Class I (*Caulobacter crescentus* (ACL95907.1), bottom α -Proteobacteria wedge). Bgxl, from *Orpinomyces* sp. strain C1A, is shown highlighted in yellow.

Figure 2. Effect of Temperature and pH on Bgxl activity A) Optimal pH, B) Optimal Temperature, C) pH Stability, D) Thermal Stability. All values are presented as relative specific activities, calculated by determining the % activity relative to the highest activity (with the highest activity set at 100%). For A, B, C, and D, PNPX was used as a substrate. Error bars represent standard deviation of triplicate (n=3) samples.

Figure 3. Substrate competition and Bgxl preference. Monosaccharides (glucose (■) or xylose (⌘)) release was assayed when Bgxl was challenged with 10 mM cellobiose (A), 10 mM xylobiose (B), or an equimolar mixture of both substrates (C). In (A), the effect of xylobiose (as a competitive inhibitor) is measured through conducting a β -glucosidase activity assay. In (B), the effect of cellobiose (as a competitive inhibitor) is measured through conducting a β -xylosidase activity assay. In (C), a competition assay was performed with both cellobiose and xylobiose present, assaying for the presence of glucose or xylose.

770 **Figure 4. Alignment of Bgxl and the four biochemically-characterized GH39-family enzymes, highlighting**
 771 **structural predictions and conservation of or around the active site.** Structural predictions for Bgxl sequence
 772 were obtained using I-TASSER three-dimensional model (Fig. S3) (Roy et al. 2010; Yang et al. 2015; Zhang 2008).
 773 Bgxl sequence is compared to those from *Caulobacter crescentus*, *Thermoanaerobacterium saccharolyticum*,
 774 *Geobacillus stearothermophilus*, and *Bacillus halodurans*. α -helices in blue are those within the small α -helical
 775 domain, α -helices and β -sheets in green are those within the $(\alpha/\beta)_8$ barrel, and β -sheets in red are those within the β -
 776 sandwich. Red stars (*) represent catalytic residues within the active site. Black stars (*) represent those residues
 777 close to the active site, as determined within the Bgxl model. Blue stars (*) represent residues noted in the
 778 literature to be important for β -xylosidase function (Czjzek et al. 2005; Yang et al. 2004).
 779

Table 1 (on next page)

Table 1

Table 1. Substrate Specificity and Specific Activity of Bgxxg1

1 **Table 1. Substrate Specificity and Specific Activity of Bgxl.**

Substrate ^a	Activity Tested	Specific Activity (U/mg ± SD)
PNPG	β-glucosidase	73.4 ± 7.15
Cellobiose	β-glucosidase	55.1 ± 5.36
PNPGal	β-galactosidase	54.6 ± 2.26
PNPX	β-xylosidase	11.5 ± 1.2
Xylobiose	β-xylosidase	10.9 ± 0.96
Beechwood Xylan	Xylanase	10.8 ± 1.25
Avicel	Exoglucanase	ND ^b
CMC	Endoglucanase	ND ^b
Locust Bean Gum	Mannanase	ND ^b
PNPA	Arabinosidase	ND ^b
PNPAc	Acetyl Xylan Esterase	ND ^b
PNPC	Cellobiohydrolase	ND ^b
PNPM	Mannosidase	ND ^b
Aldouronic acid	α-glucuronidase	ND ^b

2 **a** Abbreviations: PNPC - *p*-nitrophenyl-β-D-cellobioside, PNPX - *p*-nitrophenyl-β-D-xylopyranoside, PNPA - *p*-
3 nitrophenyl-β-D-arabinofuranoside, PNPM - *p*-nitrophenyl-β-D-mannoside, PNPG - *p*-nitrophenyl-β-D-
4 glucopyranoside, PNPGal - *p*-nitrophenyl-β-D-galactopyranoside, PNPAc - *p*-nitrophenyl-acetate.

5 **b** ND: Not detected.

Table 2(on next page)

Enzyme Kinetics for Bgxxg1

Table 2. Enzyme Kinetics for Bgxl. K_m and V_{max} values were calculated by extrapolation from Lineweaver-Burke plots.

Substrate ^a	Activity Tested	K_m ^b	V_{max} (U/mg)
PNPG	β -glucosidase	BDL ^c	769 \pm 18
PNPGal	β -galactosidase	BDL ^d	769 \pm 13
PNPX	β -xylosidase	0.00485 mM \pm 0.00062	127 \pm 8
Beechwood Xylan	Xylanase	0.038 mg/mL \pm 0.0039	25.6 \pm 10

a: Abbreviations: PNPG - *p*-nitrophenyl- β -D-glucopyranoside, PNPGal - *p*-nitrophenyl- β -D-galactopyranoside, PNPX - *p*-nitrophenyl- β -D-xylopyranoside,.

b: K_m values are expressed in either mM or mg/mL, depending on the substrate tested. Values are shown \pm standard deviation of triplicate samples (n=3).

c: BDL: Below detection limit (500 nM). Extrapolated K_m value obtained using Lineweaver-Burke plot was 0.0000125 mM \pm 0.0000096.

d: BDL: Below detection limit (500 nM). Extrapolated K_m value obtained using Lineweaver-Burke plot was 0.000214 mM \pm 0.000016.

Table 3(on next page)

Substrate competition experiments.

Table 3. Substrate competition experiments. “Activity tested” column refers to the colorimetric substrate tested (PNPX for β -xylosidase, PNPG for β -glucosidase) in the presence of the active site inhibitor (cellobiose or xylobiose, at listed Inhibitor concentrations). Specific activity, K_m , and V_{max} refer to the values calculated for the colorimetric substrate in each experiment.

Activity Tested	Active Site Inhibitor	Inhibitor (mM)	Relative Specific Activity (%)	K_m (mM)	V_{max} (U/mg)
β -xylosidase	Cellobiose	0	100	0.00485	127
		10	78.9	1.438	118
		20	52.1	3.51	129
β -glucosidase	Xylobiose	0	100	0.0000125	769
		10	75.8	0.000235	763
		20	57.2	0.00349	752

Table 4(on next page)

Comparison of key amino acids between Bgxc1 and all four biochemically characterized β -xylosidases

Table 4. Comparison of key amino acids between Bgxl and all four biochemically characterized (BC) β -xylosidases from *Thermoanaerobacterium saccharolyticum*, *Bacillus halodurans*, *Geobacillus stearothermophilus*, *Caulobacter crescentus*, as well as in Classes III-A, III-B, and III-D^a.

Pos. ^b	AA in Bgxl	AA in BC ^d	Significance of Change	Importance of Residue	Class III-A	Class III-B	Class III-C	Class III-D
46	Val	Tyr	Small, nonpolar (Val) vs. Large, polar (Tyr)	Near active site	NC ^e	Ile	Val	NC
129	Asp	Asn	Negative charge (Asp) vs. Neutral charge (Asn)	H-bonding	Lys	Asp	Asp	Asp
131 ^c	Thr/NC	Phe	Small, polar (Thr) vs. Large, nonpolar (Phe)	Near active site	NC	NC	NC	NC
139	Phe	Tyr	Large, nonpolar (Phe) vs. Large, polar (Tyr)	Near active site	Tyr	Tyr	Phe	Tyr
163	Cys	Ala	Polar, thiol (Cys) vs. Nonpolar (Ala)	Near active site	Tyr	Ala	Cys	Tyr
171	Lys	Trp	Positive charge (Lys) vs. Nonpolar (Trp)	Near active site	Trp	NC	Lys	Lys
194	Leu	Tyr	Small, nonpolar (Leu) vs. Large, polar (Tyr)	H-bonding	Ser	Ile/Glu	Leu	Tyr
242	Arg	Ala	Positive charge (Arg) vs. Small, nonpolar (Ala)	Near active site	NC	NC	Arg	NC
322-323	-gap-	Glu	Gap vs. Negative charge (Glu)	H-bonding	Arg/Thr/Lys	-gap-	-gap-	-gap-
322-323	-gap-	Glu	Gap vs. Negative charge (Glu)	H-bonding	Gly/-gap-	-gap-	-gap-	-gap-

^a No changes were identified in 10 different positions (Arg48, Ile124, Trp125, Asn126, Glu127, Pro128, Trp132, Pro162, His192, Glu225), and 5 positions were variable across all sequences (Val81, Gly130, Tyr164, Ser165, Lys247).

^b Pos. (Positions) refer to the position of the amino acid in Bgxl

^c Bgxl and all proteins in Class III-C β -xylosidases have identical amino acid sequences in all key positions with one exception (Thr131)

^d Sequences identified using the alignment presented in Fig. 5.

^e NC = Not conserved

Figure 1(on next page)

Phylogenetic analysis of GH39 β -xylosidases, including Bgxxg1.

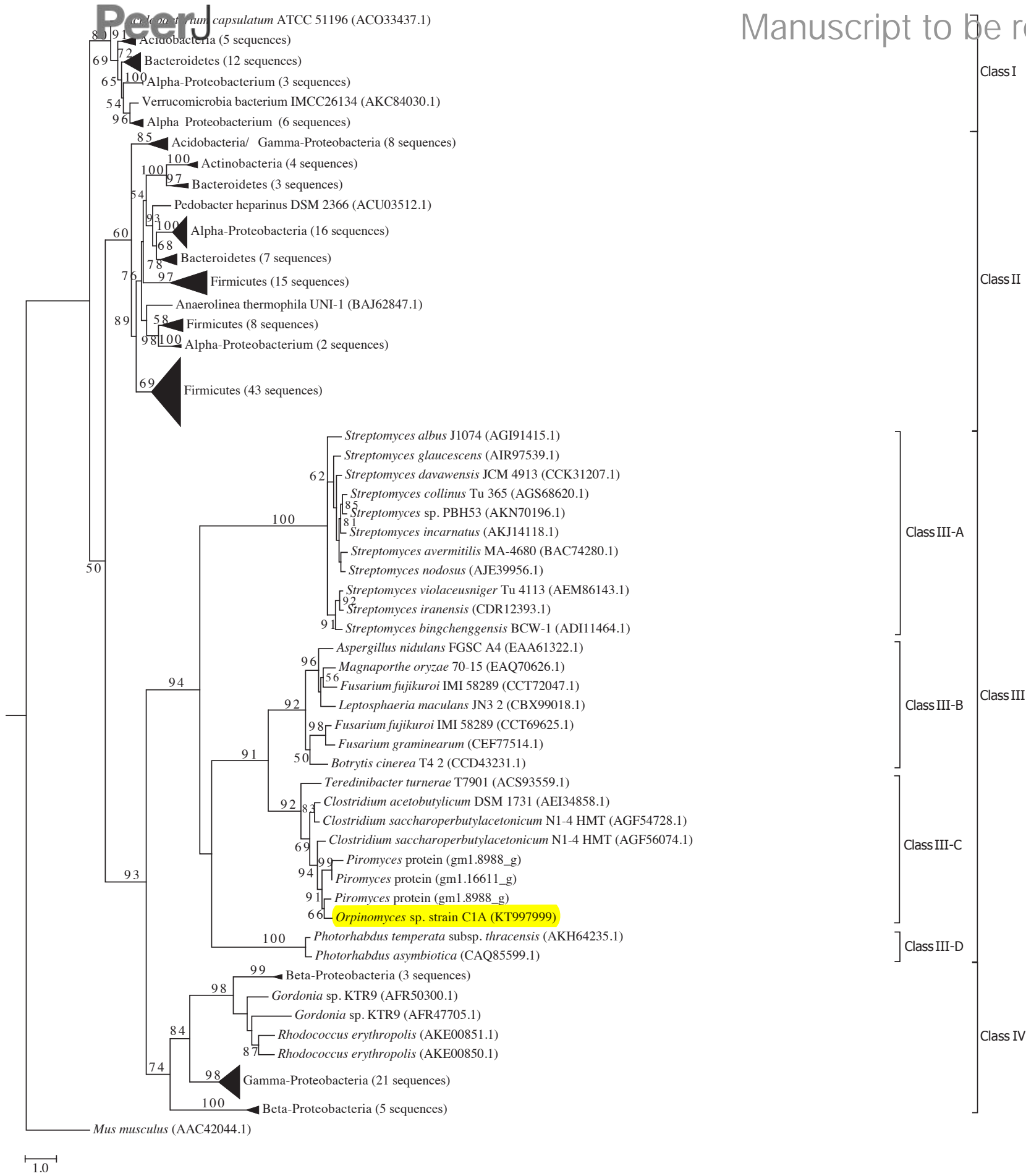
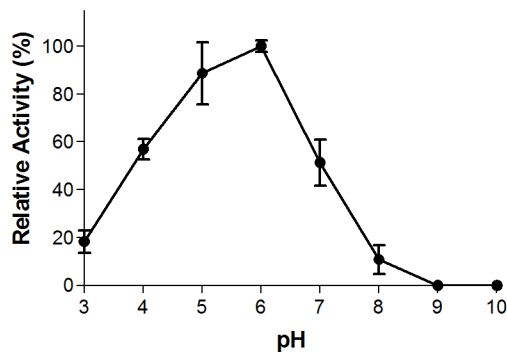


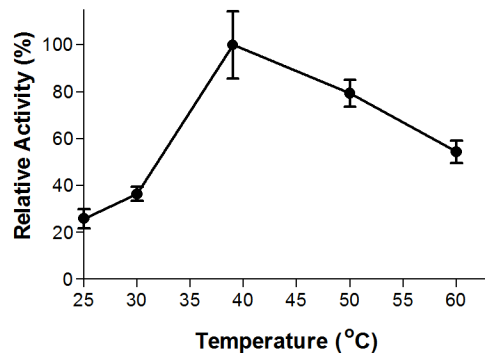
Figure 2(on next page)

Effect of Temperature and pH on Bgwg1 activity A) Optimal pH, B) Optimal Temperature, C) pH Stability, D) Thermal Stability

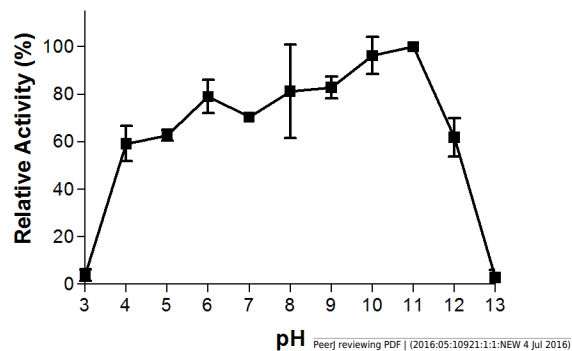
A



B



C



D

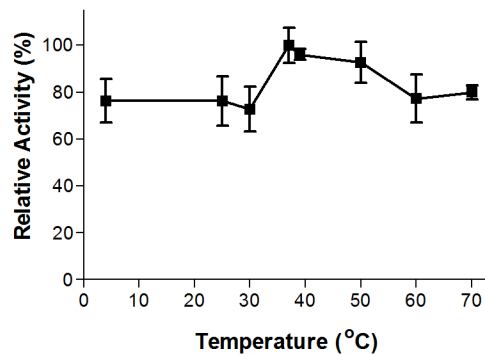


Figure 3

Alignment of Bgxxg1 and the four biochemically-characterized GH39-family enzymes, highlighting structural predictions and conservation of or around the active site.

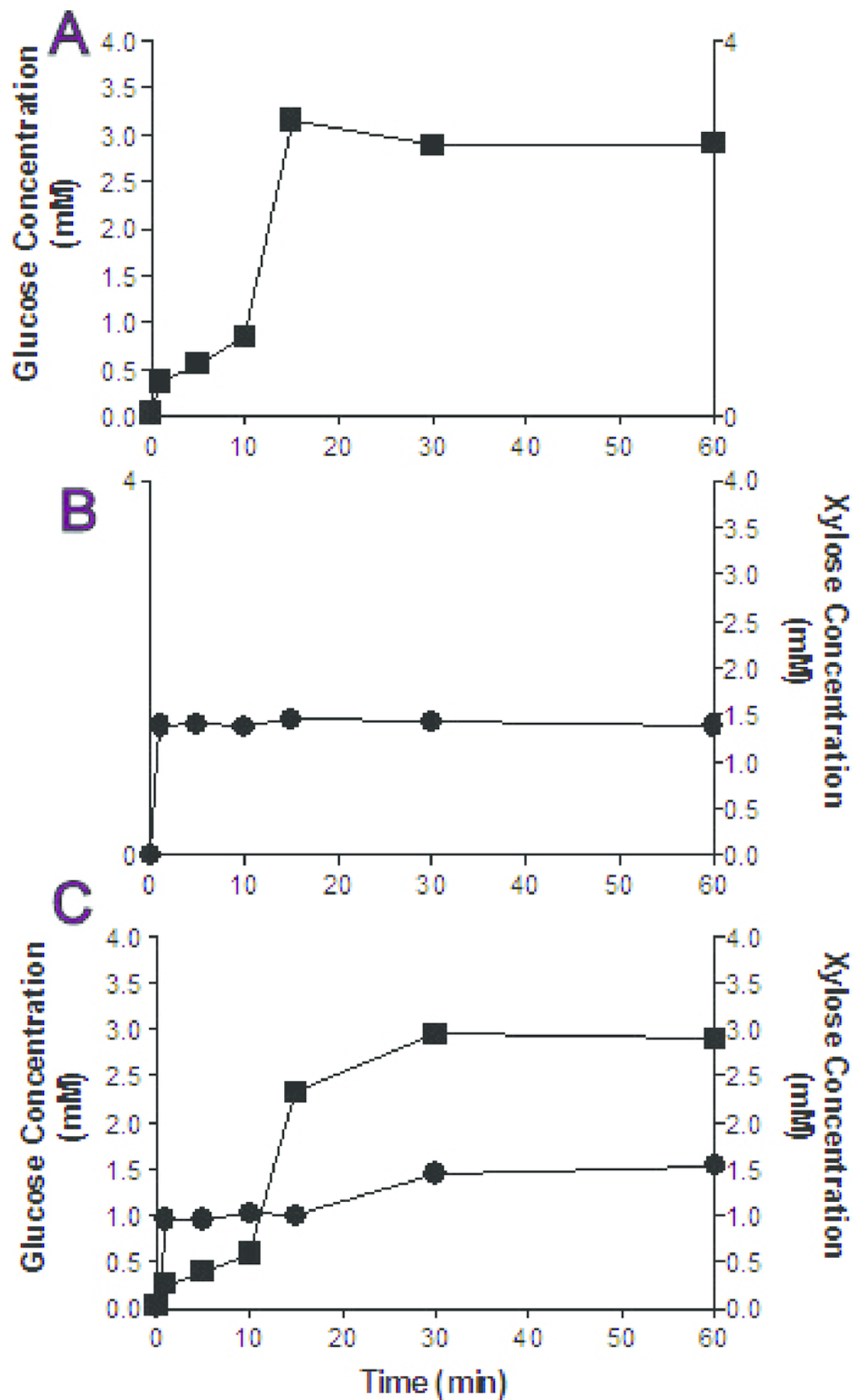


Figure 4(on next page)

Alignment of Bgxxg1 and the four biochemically-characterized GH39-family enzymes, highlighting structural predictions and conservation of or around the active site.

Bgxcg1	1	MT.....NVLTVE...CNNKL.RRATHCANGSLYGIT..ETTPRDYKNLVDP LHPFVMRN.....PARGGNG	
Caulobacter	1	MANAGPGARVIDLDL RRAAGPVDRFFDLSIGSDYPGTLIREDSQAQLKTTVDELGFYIRFHAIFHDVLGTVKVQ.....	
Thermoanaerobacterium	1	MIKVRVP.DFSDKKFSDRWRYCVGTGRLGLALQKEYIETLK YVKENIDFKYIRGHGLLCDDVGIYRED.VVGD	
Geobacillus	1	MKVVNVP.SNGREKFKKNWKFCVGTGRLGLALQKEYLDHLKLVQEKIGFRYIRGHGLLSDDVGIYREV.EIDG	
Bacillus	1	MKTVVVN.DRSFAYFPKKWKYCIGTGRLGLALQKEYVDHLARLQKELNFQYIRGHGLLHDDIGIYRERKRADG	
			<div>α-4</div> <div>β-2</div> <div>α-5</div>
Bgxcg1	57	NQHPYGDAL.....KVARRLADTPGALVSVDLPDMLPGWPYKWPG.....MQNWLNQVKFSFI....KDK	
Caulobacter	76	DGKIVYDWTKIDQLYDAL LAKGIKPFIELGFTPEAMKTSDQ.....TIFYWKGNTSHPK.LGPWRDLIDAFVHHLRARY	
Thermoanaerobacterium	72	EVKPFYNFTYIDRIFDSFLEIGIRPFVEIGFMPKKLASGTQ.....TVFYWEGNVTTPPKDYEKWSDLVKAVLHHFISRY	
Geobacillus	72	EMKPFYNFTYIDRIVDSYLALNIRPFIEFGFMPKALASGDQ.....TVFYWKGNVTTPPKDYNKWRDLIVAVVSHFIERY	
Bacillus	73	TVEPFYNFTYIDRIFDTFLELNIRPFVEIGFMPKKLASGEQ.....TIFDWQGNVTTPPKDYDQWKQLIQAVISHFIDRY	
			<div>α-5</div> <div>β-3</div> <div>α-6</div> <div>β-4</div> <div>α-7</div> <div>β-5</div>
Bgxcg1	112	KASGLKNWYGLEIWNEDP..GTWNNSN.GSFEEMWKQTYQAI RQADPNEKIIGPCYSWYTD DKLNRNFLKYAKANNCLPDI	
Caulobacter	149	GVEEVRTW.FFEVWNEPNLDGFW EKADQAAYFELYDVTARAIK AIDPSLRVGGPATAGA..AWVPEFLAHVKKSGSAVDF	
Thermoanaerobacterium	146	GIEEVLKW.PFEIWNENPNLKEFWKDADEK EYFKLYKVTA KAIKEVNENLK VGGPAICGGADYWI EDFLNF CYEENVPVDF	
Geobacillus	146	GIEEVRTW.LFEVWNEPNLVNFWKDANKQEYFKLYEVTARAVKSVDPHLQVGGPAICGGSD EWI TDFLHFC AERRVPVDF	
Bacillus	147	GVEEVTKW.PFEIWNENPNLINFWQHADKKE YFKLYK I TARA IKEVHPYIQVGGPAICGGSD EWI TDFLQ FCHKEEVPVDF	
			<div>β-5</div> <div>α-8</div> <div>β-6</div> <div>α-9</div>
Bgxcg1	189	ISWHELSGI.....DGVSSHLSYREIEKSLGIP ELPISINEY CDAKHELEGQPG..SSARF IG.KF	
Caulobacter	226	VTTHTYGV DGGFLDEKGVQDTKLSPSPDAVVGDVRRVREQIEASAFPGLPLYFTEWSTSYTPRDSVHDSYVSAAYIVEKL	
Thermoanaerobacterium	225	VSRHAYTSKQG.EYTPHLIYQEIMP.SEYMLNEFKTVREI IKNSHFPNLPFHITEYNTSYSPQNPVHDTPFNAAYIARIL	
Geobacillus	225	VSRHAYTSKAPHKKTFEYY YQELEP.PEDMLEQFKTVRALIRQSPFPHLP LHITEYNTSYSPINP I HDTALNAAYIARIL	
Bacillus	226	VSRHAYTSAPHKVTPDYY YQELYE.NTHMLDELKSVKELIQQSPFPNLPFHITEYNTSYSPINPVHDTVLNAAYLARIL	
			<div>α-9</div> <div>β-7</div> <div>α-10</div> <div>β-8</div> <div>β-9</div>
Bgxcg1	248	ERYKV.DTAMITWVFV.....PLPGRLGSL LATDTQKGAGWYFYK WYGDMTGDMVYVKPPNDNSNLVDGAACVD	
Caulobacter	306	RRVKGLVQAMSYWTYSDLFEEPGPPTAPFQGGFG.LMNPQGIRKPSWFAYKYLNALKGRELVCADDQVFAARDGDRVA..	
Thermoanaerobacterium	303	SEGGDYVDSFSYWTFSDVFEEERDVP RSQFHGGFG.LVALNMIPKPTFYTFKFFNAMGEEMLYRDEHMLVTRR DGSVA..	
Geobacillus	304	SEGGDYVDSFSYWTFSDVFEEEMDVPKALFHGGFG.LVALHSIPKPTFHAF TFFNALGDEL LYRDGEMIVTRRK DGSIA..	
Bacillus	305	SEAGDI VDSFSYWTFSDVFEEAGVPTAPFHGGFG.LIALHGIAKPTYHLFSFFNQ LGEQLLYRDSQM VTKKQDGSIQ..	
			<div>β-10</div> <div>β-11</div>
Bgxcg1	316	TNKEYISFIFGGPNDGTI.RASSIIFQALLDLLPML	
Caulobacter	383IVAYAWRQPDQKVSNRPFYTKLHPASDVEPLKVRLTSLKPGRYKLRVRRVGYRRNDAYSAYIDMGSP TTTLTESQLQ	
Thermoanaerobacterium	380LI..AWNEMDKTENPDEDYEVE.....IPVRF.....RDVFIKRQLIDEEHGNPWGTWIMGRPRYP SKEQVN	
Geobacillus	381AV..LWNLMKGE GFTKEVQLV.....IPVSF.....SAVFIKRQIVNEQYGNARVWKQMGRPRFP SRQAVE	
Bacillus	382LV..VWNLMKGEGLEQTVQIE.....LPTQS.....DAVFIKRKTIDE TNGNPWRVWKE MGRPRFPKKNEID	
Bgxcg1	351		
Caulobacter	459	SLQALTEDRPEIEKALKVSGETVVDLPMRAN DVVLIELEPLA	
Thermoanaerobacterium	442	TLREVAKPEIMTSQPVANDGYLNLKFKLGKN AVVLYELTERIDESSTYIGLDDSKINGY	
Geobacillus	443	TLRQVAQPHVMTEQRRATDGVIIHLSIVLSKNEVT LIEIEQVRDETSTYVGLDDGEMTSYSS	
Bacillus	444	TLQEAQPLIRTERRDGLSRTLKLELTL SKNEVSLVEVFPIIDETNTYPGLDDRLIPSY	